A PROPOSED MECHANISM OF [*closo*-$CB_{11}H_{12}$]$^-$ FORMATION BY DICHLOROCARBENE INSERTION INTO [*nido*-$B_{11}H_{14}$]$^-$. A COMPUTATIONAL STUDY BY DENSITY FUNCTIONAL THEORY

Pawel REMPALA[1] and Josef MICHL[2,*]

Department of Chemistry and Biochemistry, University of Colorado, Boulder, CO 80309-0215, U.S.A.; e-mail: [1] rempala@eefus.colorado.edu, [2] michl@eefus.colorado.edu

Received November 15, 2002
Accepted November 20, 2002

Dedicated to Professor Petr Čársky on the occasion of his 60th birthday in recognition of his major contributions to quantum chemistry.

A plausible mechanism is proposed for the insertion of dichlorocarbene into [*nido*-$B_{11}H_{14}$]$^-$ to yield [*closo*-$CB_{11}H_{12}$]$^-$ and is supported by the results of density functional theory and *ab initio* calculations.

Keywords: Boranes; Boron clusters; Carboranes; Carbenes; Reaction mechanisms; Density functional calculations; DFT calculations; *Ab initio* calculations.

The deltahedral carborane anion, [*closo*-$CB_{11}H_{12}$]$^-$ (**1**), and its derivatives are of considerable interest because of their very low nucleophilicity[1–3], but until a short time ago were expensive to prepare. A recent two-step synthesis from $NaBH_4$ and BF_3 etherate *via* the [*nido*-$B_{11}H_{14}$]$^-$ anion (**2**) in a 20% overall yield has made the parent anion more readily available[4] (Scheme 1). The second step in the sequence is an insertion of dichlorocarbene into the deprotonated form of **2**, the [*nido*-$B_{11}H_{13}$]$^{2-}$ dianion (**3**). The use of carbenes for the insertion of a carbon atom into a borane cage is new and appears to have some generality in that several different carbenes and boranes have been used successfully[4,5]. We now wish to propose a rational explanation of this reaction in the form of a mechanistic scheme that is consistent with the observed appearance of side products and is backed by density functional theory (DFT) and *ab initio* calculations. The computational results are only tentative, primarily because solvent effects are severely approximated, but are useful in that they suggest further kinetic and other mechanistic experiments.

doi:10.1135/cccc20030644

METHOD OF CALCULATION

The B3LYP functional[6–8] in conjunction with the 6-31G(d,p) basis set[9–13] was used as the main computational tool, and all computational results listed refer to it unless stated otherwise. The MP2/6-31G(d,p) method was used to verify that the nature of crucial stationary points does not depend on how electron correlation is treated. Two other functionals, BHandHLYP[14] and BLYP[7,14–16], were also tested in some instances, with similar results. All calculations were performed using the Gaussian 98 software[17] running on Pentium dual processor Linux computers and an Exemplar S2200 Hewlett–Packard workstation. Natural bond orbital analysis[18,19] of atomic charges, as implemented in Gaussian 98, was performed on selected structures. Solvent influence was approximated by the Onsager model[20,21] (tetrahydrofuran, ε = 7.58), using Gaussian 98 software. Relative energies (reaction barriers and reaction energies) reported in the text include zero-point energy (ZPE) and solvation corrections (inclusive of the monopole energy term), unless stated otherwise.

Structures of initially guessed intermediates were subjected to geometry optimizations and vibrational analysis. Next, an attempt was made to find first-order transition states that connect structures verified as energy min-

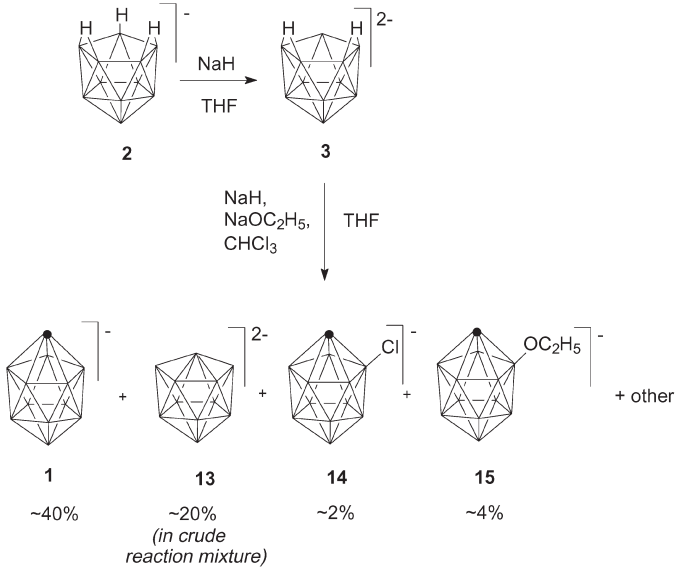

SCHEME 1
Synthesis of **1**[4]. In all schemes, a vertex stands for the BH group, unless it is marked by a dot, which stands for a CH group

ima. The nature of the imaginary mode was inspected, and whenever there was doubt as to which minima the transition state connects, its structure was distorted slightly along the imaginary mode vector in both directions and optimized. Sometimes the procedure led to unexpected minima. These new stationary points were added to the reaction scheme and additional transition states were searched, until a consistent reaction path was established.

RESULTS

The dichlorocarbene insertion reaction (Scheme 1) is performed by first deprotonating the sodium salt of the [*nido*-$B_{11}H_{14}]^-$ anion (**2**) with NaH in tetrahydrofuran and then adding $CHCl_3$ in the presence of excess strong base (typically NaH and/or C_2H_5ONa). Under these conditions, $CHCl_3$ is known to be deprotonated to CCl_3^-, which then loses the Cl^- anion to yield dichlorocarbene ($:CCl_2$)[22,23], and we shall assume that this carbene is the actual reagent. We further make the assumption that the strongly basic [*nido*-$B_{11}H_{13}]^{2-}$ dianion (**3**) performs a nucleophilic addition to the carbon of $:CCl_2$, triggering a sequence of events that involve the removal of an additional proton by the excess base present and a loss of two chloride anions, and ultimately yield the [*closo*-$CB_{11}H_{12}]^-$ anion (**1**). The insertion reaction is accompanied by the formation of byproducts. Some of these have been identified (Scheme 1), and their significance will be discussed below.

Unless specified otherwise, all computed energies refer to the B3LYP/6-31G(d,p) level of theory and include zero-point energy and solvent effects. For details, see Table I.

Deprotonation of [*nido*-$B_{11}H_{14}]^-$ (**2**)

Two structures, **2a** and **2b**, were found for the isolated anion **2** (Fig. 1). In vacuum, **2b** is 0.1 kcal/mol less stable than **2a** if ZPE is not included, and very slightly more stable if it is. Both isomers possess C_s symmetry and show no imaginary frequencies in analytical vibrational analysis. The difference between the structures is the number of hydrogen atoms involved in B···H···B bridges (two in **2a** and three in **2b**, Scheme 2). The addition of diffuse functions on boron (B3LYP/6-31+G(d,p)) does not cause a significant change in the calculated geometries. So far only structure **2a** has been described in the literature as corresponding to an energy minimum, by X-ray diffraction analysis of solid PMe_3H^+[*nido*-$B_{11}H_{14}]^-$ [24], and by a

HF/3-21G calculation[25]. At this rather modest level of theory the structure **2b** was a transition state for a circulation of the three hydrogens around the top rim of the cage. In the MP2/6-31G(d,p) approximation, the two-bridge structure **2a** is higher in energy than the three-bridge structure **2b** by about 1 kcal/mol (vacuum, no ZPE) and is a first-order transition state (imaginary frequency 228*i* cm^{-1}). The very small calculated energy differences between the two structures in all of these approximations are compatible with the observed[25] fluxional nature of the hydrogens in **2**, but do not allow us to reach a conclusion about the actual minimum energy structure, particularly in solution. This is irrelevant for our purposes.

The computed heat of deprotonation of isolated **2** to yield the dianion **3** (the proton affinity of **3**) is very high, 420.6 kcal/mol (see Table I). The solution affinity of **3** for the solvated proton, THF·H^+, is 88.4 kcal/mol, including one THF molecule explicitly. We do not wish to dwell on the deprotonation step, since conversion of **2** to **3** under the reaction conditions is not in doubt, based on ^{11}B NMR spectra, and calculations on

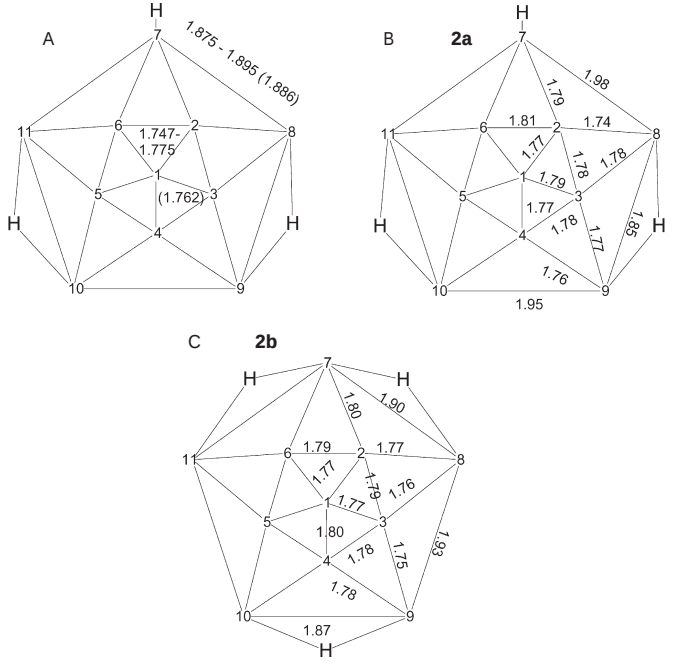

FIG. 1

Geometry of **2**: A, experimental X-ray structure[24]; B and C, B3LYP structures of **2a** and **2b**, respectively. Selected interatomic distances in Å, average values in parentheses

dianions isolated in the gas phase have limited credibility (spontaneous electron detachment is possible).

Addition of $:CCl_2$ to [*nido*-$B_{11}H_{13}$]$^{2-}$

Dihalocarbenes are nearly exactly ambiphilic[26,27] and can react both as electrophiles and nucleophiles; for dichlorocarbene the electrophilic character prevails. In order to gain insight into the properties of the dianion **3** as a nucleophile, we performed an NBO analysis[18,19] of natural atomic charges based on the calculated density (Fig. 2). Boron atoms generally ex-

TABLE I
Relative energies (kcal/mol) of the species listed in Scheme 2[a]

Species[b]		Gas phase (no ZPE)	Gas phase (ZPE)	Solution (ZPE)
$B_{11}H_{14}^-$, $B_{11}H_{13}^{2-}$	**2a**	0	0	0
	3	428.3	420.6	328.0
$B_{11}H_{13}CCl_2^{2-}$	**4**	0	0	0
	TS(4–6)	3.5	1.4	1.4
	TS(4–5)	4.2	3.7	3.0
$B_{11}H_{13}CCl^-$, $B_{11}H_{12}CCl^{2-}$	**5**	0	0	0
	6	7.1	8.0	9.0
	TS(6–5)	33.2	30.5	32.4
	6t = TS(6–6)	12.2	13.1	13.9
	8	418.9	410.7	325.1
	9	422.4	414.0	325.0
	TS(8–10)	433.6	424.3	332.7
	TS(9-11)	435.5	426.3	342.6
$B_{11}H_{12}C^-$, $B_{11}H_{11}C^{2-}$	**1**	0	0	0
	10	88.2	84.3	83.6
	11	103.6	99.0	98.9
	TS(11–10)	107.0	101.7	101.8
	12	478.7	468.7	376.9

[a] ZPE, zero point energy. [b] Only species of the same composition or differing by a proton can be compared directly.

hibited negative charges while hydrogens were nearly neutral, with the notable exception of the two bridge B···H···B hydrogens. Significantly, the boron atom at which deprotonation took place showed the largest negative charge, and even its remaining hydrogen became slightly negative (–0.011). The average charge for the five boron atoms at the cage opening is –0.251, while the average charge for the five-membered boron ring beneath the opening is –0.202, and the boron atom at the bottom carries a charge of –0.206. The distribution of the highest occupied molecular orbital (HOMO) in the dianion is apparent from its contributions to the natural atomic

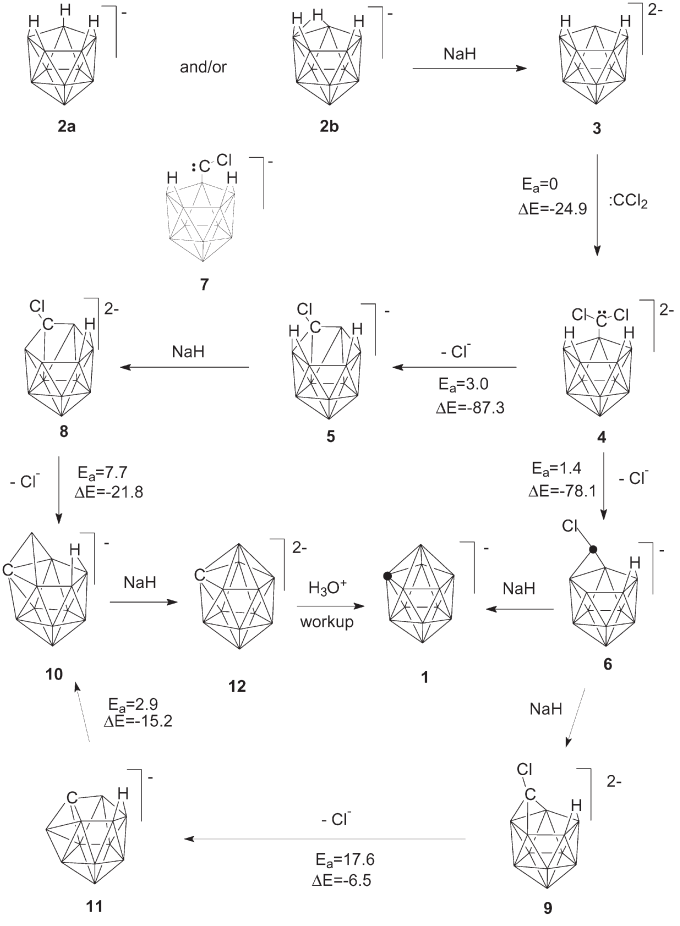

SCHEME 2

The proposed mechanism for the conversion of **2** to **1**. B3LYP/6-31G(d,p) calculated reaction energies and activation barriers (ZPE and solvation included) are given in kcal/mol

charges, also shown in Fig. 2. It seems safe to assume that :CCl_2 acts as an electrophile towards this dianion reaction partner, attacking **3** with its empty orbital on carbon in position 7, where a proton would also attack, and where we calculated the highest negative charge. Such a step should lead to B–C bond formation and to the generation of the dianion **4**.

At both the B3LYP/6-31G(d,p) and the MP2/6-31G(d,p) levels of calculation **4** is an energy minimum. The lowest calculated frequencies are 60 and 78 cm^{-1}, respectively. The calculated charge distribution in this dianion is shown in Fig. 3, and agrees with expectations based on formula **4**. The carbon atom and its two chlorine substituents carry large negative charges, and the $–CCl_2^-$ group thus carries almost exactly one negative charge, while the other is delocalized in the boron cage. The carbene insertion reaction is calculated to be exothermic by 24.9 kcal/mol, including one explicit THF molecule to account for ylide formation with :CCl_2 (37.9 kcal/mol without solvent). A relaxed energy scan along the B–C distance coordinate does not indicate the presence of an energy barrier for the carbene addition step, neither in the gas phase nor in solution.

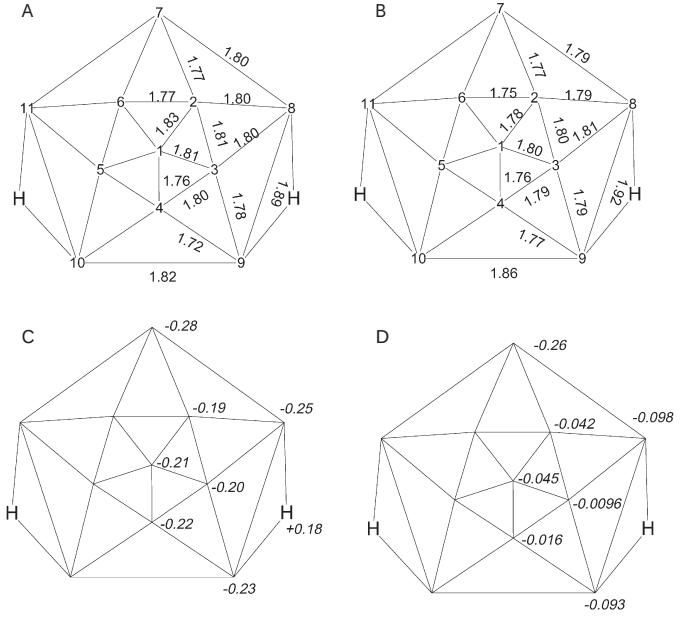

FIG. 2

Geometry of **3**: A, experimental X-ray structure[28]; B, B3LYP structure; C, B3LYP NBO charges; D, B3LYP NBO contributions to atomic charges from HOMO. Selected interatomic distances in Å, charges in elementary charge units

α-Elimination of the First Chloride Anion to Form [*nido*-$CB_{11}H_{13}Cl$]$^-$ (**5** or **6**)

An α-elimination of Cl^-, a good leaving group, from **4** appears as likely as the initial α-elimination from CCl_3^- that yielded $:CCl_2$. By analogy, it should initially lead to a new carbene (**7**), [*nido*-$B_{11}H_{13}$-:C–Cl]$^-$. However, this hypothetical carbene, also shown in Scheme 2, does not appear to have independent existence. Although calculations at the more approximate HF/6-31G(d,p) level predict that **7** is metastable, efforts to locate such an energy minimum under C_s symmetry constraint at a correlated level failed, using the MP2 method and several density functionals (B3LYP, HandHLYP, BLYP). MP2 geometry optimizations with imposed C_s symmetry led to abstraction of two hydrogen atoms by the divalent carbon and formation of a chloromethyl group. This process was not examined further. Energy minimization with DFT methods under C_s symmetry constraint always led to stationary points at structures with the carbon atom inserted between two boron atoms, and with one a″ mode of an imaginary frequency. Subsequent removal of the symmetry constraint led to structure **5**, located 87.3 kcal/mol below **4** – Cl^- (119.3 kcal/mol in the gas phase).

When the non-stationary geometry obtained from **4** by removal of Cl^- was optimized without the C_s constraint, starting at a carbene-like structure close to C_s symmetry, geometry optimization led directly to **5.** The transition state that leads from **4** to **5** (Fig. 4) is early, has one imaginary frequency, 221*i* cm^{-1}, and a barrier of 3.0 kcal/mol.

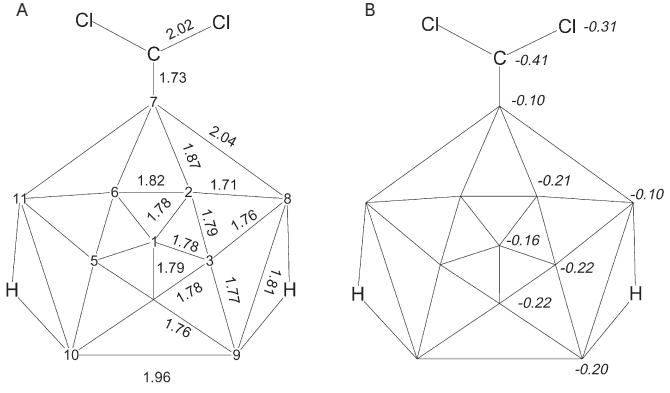

FIG. 3
Geometry of **4**: A, B3LYP structure; B, calculated NBO charges. Selected interatomic distances in Å, charges in elementary charge units

In contrast, optimization of the C_1 non-stationary point obtained from **4** by removal of Cl^- leads to **6**, the product expected when the carbene inserts between the adjacent B and H atoms of the B···H···B bridge (this starting point is a rotamer of **7** in which the remaining chlorine atom does not lie near the symmetry plane of the cage). The overall process is exothermic by 78.1 kcal/mol (111.0 kcal/mol in vacuum). A search for the transition state for this process starting with **4** resulted in a slightly asymmetric structure (Fig. 5) with one C–Cl distance (the leaving Cl^-) at 2.09 Å, and the other, at 1.93 Å. The C–H distance is 1.59 Å. The single imaginary frequency mode ($1012i$ cm^{-1}) fits expectations for motion from **4** to **6**, and the calculated barrier is 1.35 kcal/mol. An alternative C_s structure of **6**, with the C atom

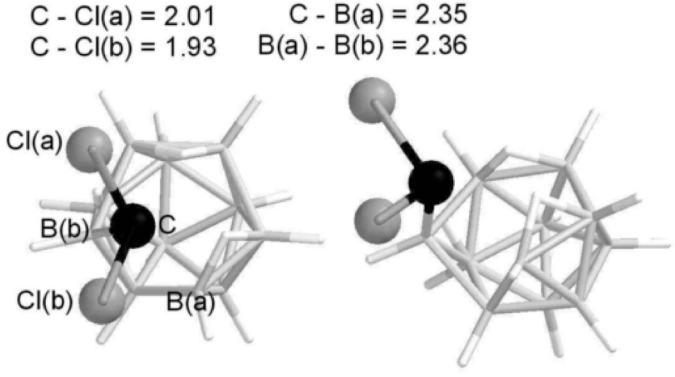

FIG. 4
Transition state for the reaction **4** → **5** + Cl^-. Selected interatomic distances in Å

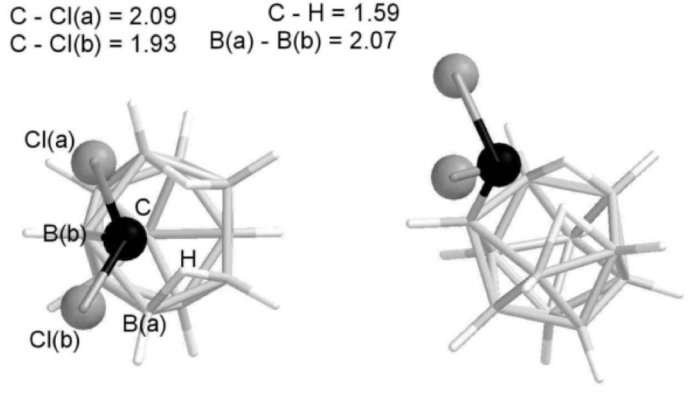

FIG. 5
Transition state for the reaction **4** → **6** + Cl^-. Selected interatomic distances in Å

coordinated to three B atoms, lies 4.9 kcal/mol higher. It is a transition state **6t** (172*i* cm^{-1}) for a degenerate **6** to **6** rearrangement (Scheme 3).

It thus appears that **4** readily produces both the anion **5** and the anion **6**, which is formed with a smaller activation energy but is 9.0 kcal/mol less stable than **5**, as the next intermediates on the reaction path towards **1**. The rearrangement of **5** to **6** requires overcoming a 32.4 kcal/mol energy barrier, and this interconversion cannot be significant (Fig. 6 shows the structure of this transition state). We have not found any other products derived directly from **4**, but cannot exclude their existence. However, B–B and B–H insertions appear to be the two logical options.

Deprotonation of [*nido*-$CB_{11}H_{13}Cl$]$^-$ (**5** or **6**)

Deprotonation of **5** by removal of either of the two bridge hydrogen atoms leads to the dianion **8**. One of the processes is straightforward (Scheme 2).

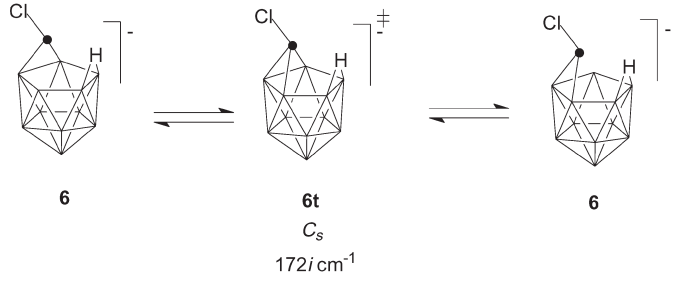

SCHEME 3
Degenerate rearrangement of **6**

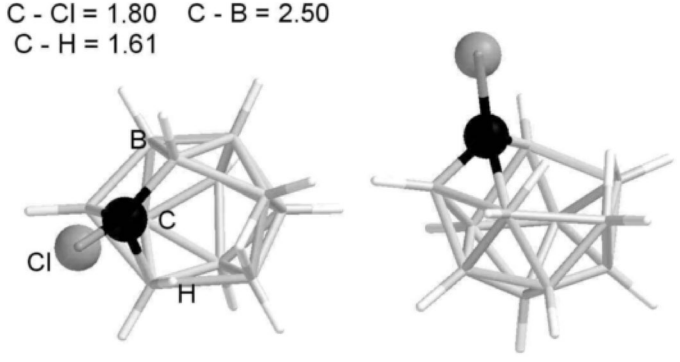

FIG. 6
Transition state for the rearrangement of **5** to **6**

In the other, the remaining hydrogen bridge migrates during the optimization and a mirror image of the formula **8** shown in Scheme 2 is formed. The affinity of **8** for a solvated proton is calculated to be 85.5 kcal/mol, very close to the 88.4 kcal/mol value calculated for **3**. This implies that the deprotonation of **5** should be just as feasible as that of **2**.

In **6**, the proton geminal to the chlorine atom clearly is the most acidic, and we first examined deprotonation in this position. The proton affinity of the conjugate dianion **9** in the gas phase (with **6** as a product) is calculated to be 406.0 kcal/mol, lower than the 420.6 kcal/mol calculated above for the dianion **3**. In solution the affinity of **9** for the solvated proton, $THF{\cdot}H^+$, is estimated to be 76.5 kcal/mol (*cf.* 88.4 kcal/mol for $B_{11}H_{13}^{2-}$).

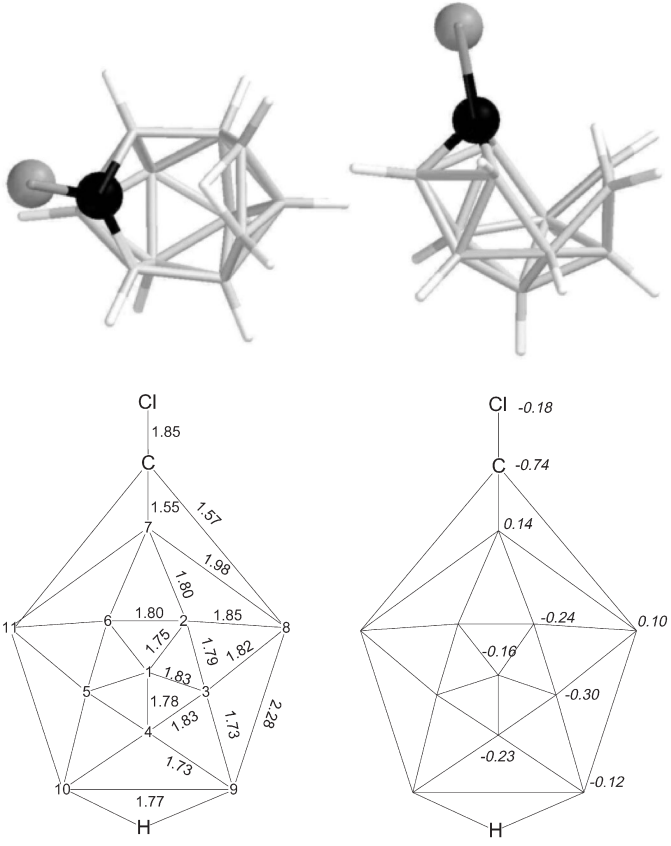

FIG. 7

Geometry of **9**: B3LYP structure and calculated NBO charges. Selected interatomic distances in Å, charges in elementary charge units

Since under the reaction conditions the deprotonation of **2** is quantitative, there is little doubt that any **6** that is formed will be deprotonated as well. The resulting dianion **9** is calculated to be an energy minimum with three B atoms coordinated to the C atom, which remains connected to its Cl substituent. The structure **9** and its charge distribution are presented in Fig. 7. Two of the B–B distances at the cage opening are rather long.

The acidity of the hydrogen bridges of **5** suggests that the second most acidic hydrogen in **6** would be the one bridging two boron atoms. Removal of this proton from **6** followed by geometry optimization led to chloride loss and formation of **1**. To determine whether this direct step from **6** to **1** is competitive with the deprotonation of **6** at carbon would require a determination of their relative kinetic acidity towards solid NaH, which is hard and was not attempted here.

α-Elimination of the Second Chloride Anion to Form [*iso*-$CB_{11}H_{12}$]$^-$ (Anions **10** or **11**)

α-Elimination of Cl^- from **8** and **9** appears likely. A search for the corresponding transition state yielded a structure connecting **8** with **10** (Fig. 8). The activation energy is 7.7 kcal/mol (13.5 kcal/mol in vacuum). Dissociation of Cl^- from **9** might be anticipated to yield a carbene, but once again, this does not appear to have independent existence and collapses to **11**, an isomer of **1**. The reaction barrier is calculated to be 17.6 kcal/mol (12.2 kcal/mol in vacuum). The structure of the transition state connecting **9** and **11** is shown in Fig. 9, and that of the intermediate **11** in Fig. 10.

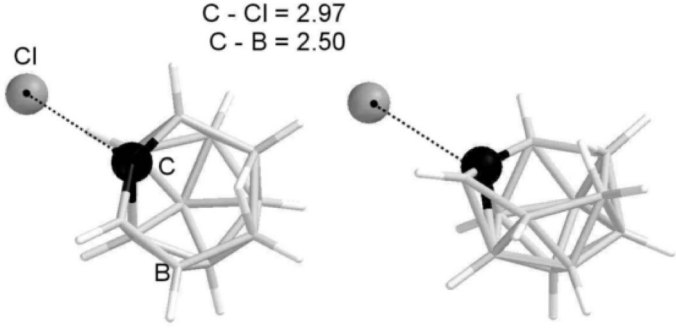

FIG. 8
Transition state for the reaction **8** → **10** + Cl^-

Rearrangement of **11** to **10**

The peculiar geometry of **11** suggests that it might be susceptible to rearrangement. Indeed, the barrier to rearrangement to **10**, which primarily involves the motion of one BH vertex, has a very low barrier (2.9 kcal/mol in solution and 2.7 kcal/mol in vacuum). The transition state lies approximately in the middle between the structures **11** and **10** (Fig. 11). The rearrangement is exothermic by 15.2 kcal/mol. Thus, the reaction branching initiated with two possible products (**5** and **6**) from **4** converges to a common intermediate, **10**.

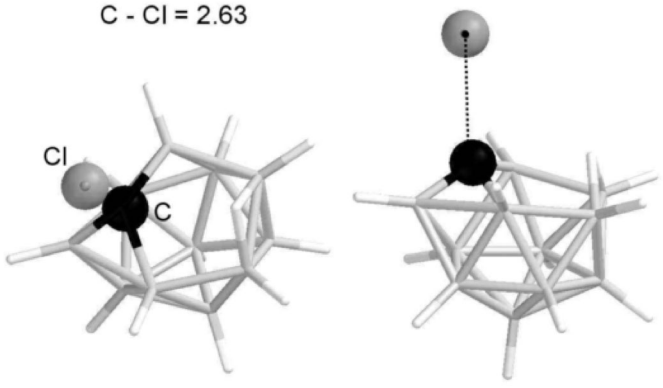

FIG. 9
Transition state for the reaction **9** → **11** + Cl^-

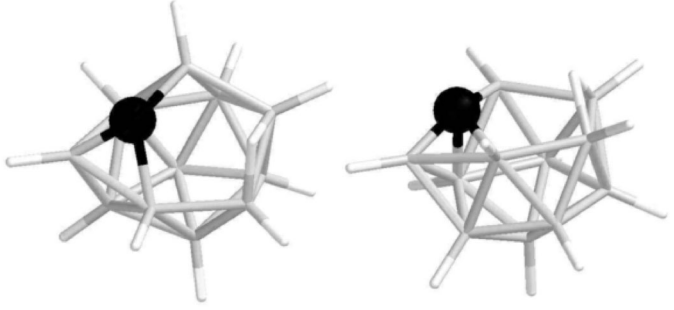

FIG. 10
B3LYP geometry of **11**

Isomerization of [*iso*-$CB_{11}H_{12}$]$^-$ (**10**) to **1**

Compound **10** is an isomer of **1**, and differs from **1** by a different placement of one hydrogen atom (Fig. 12). The two species share a common conjugate base, the dianion **12**, and the deprotonation of **10** at the hydrogen bridge followed by geometry optimization leads to **12**. The isomer **10** is 83.6 kcal/mol less stable than **1**, and reprotonation by protic work-up will turn **12** into the final product **1**. The affinity of **12** for a solvated proton, *i.e.*, protonation leading to **1**, is calculated to be 137.3 kcal/mol, and it is the strongest base considered presently.

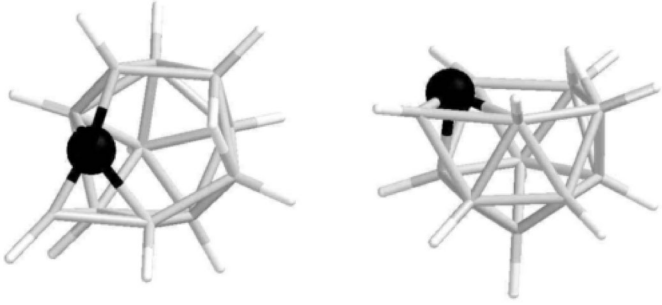

FIG. 11
Transition state for the rearrangement of **11** to **10**

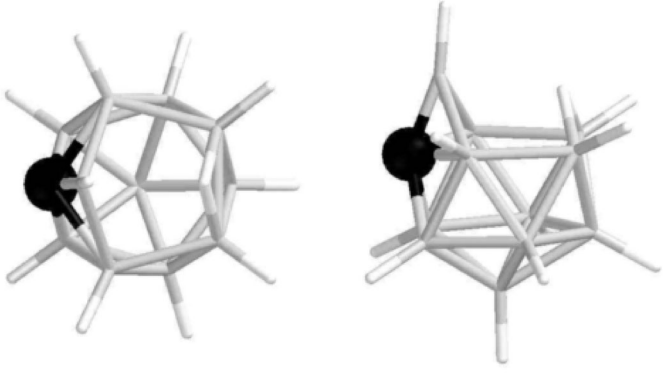

FIG. 12
B3LYP geometry of **10**

Side Reactions

1. Oxidation. Under the reaction conditions a significant fraction of the *nido* dianion **3** is oxidized to the [*closo*-$B_{11}H_{11}$]$^{2-}$ (**13**) dianion (Scheme 1). This process, presumably initiated by electron transfer to $CHCl_3$, is more important when $CHBr_3$ is used instead, and is the dominant reaction when CHI_3 is used[4]. We have made no attempt to examine its mechanism.

2. Substitution. The formation of small amounts of 2-substituted derivatives, **14** and **15**, as byproducts[4] (Scheme 1) provides a useful hint about the reaction mechanism. These products clearly result from an attack by a nucleophile such as ethoxide or chloride in a position that is very unreactive towards such attack in **1** itself. If trimethylamine is added deliberately into the reaction mixture, the zwitterion 2-Me_3N^+-*closo*-$CB_{11}H_{11}^-$ (**16**) is formed[4] instead of **1**. When $CHBr_3$ is used in the reaction instead of $CHCl_3$, 2-Br-**1** is formed[4] in addition to **1**. The 2-substituted derivatives of **1** must originate from an nucleophilic attack not at **1** but at an intermediate that occurs earlier in the reaction path. A plausible reaction mechanism therefore must contain such an intermediate.

In the reaction scheme proposed presently, the dianions **8** and **9** are likely to accumulate, but a nucleophilic attack on a dianion is probably difficult. Then, the monoanions **5** and **6** are the logical suspects. As a reaction of a nucleophile bearing a negative charge with an anion would be problematic to model in the gas phase (or in a low dielectric constant solvent, such as tetrahydrofuran) due to Coulombic repulsions, we simulated the reactions of **5** and **6** with trimethylamine (Scheme 4). Exploration of NMe_3

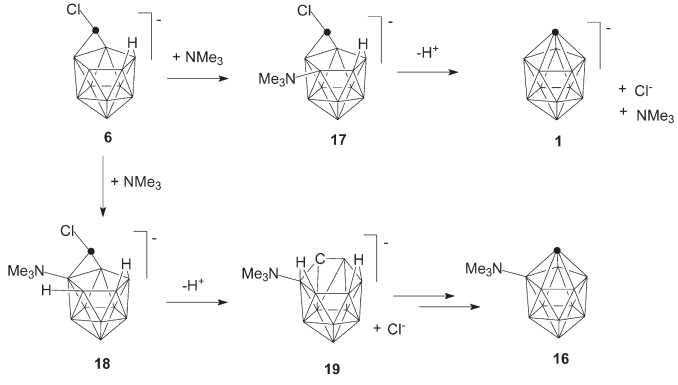

SCHEME 4
Nucleophilic trapping of **6**

adducts to **5** led to a loss of the nucleophile in the course of geometry optimization. Therefore, **5** does not seem to be the intermediate needed to explain side-product formation. Similarly, the nucleophile could not be attached to the most positively charged B atom of **10**. According to an NBO analysis, this is the boron located next to the carbon atom and adjacent to the bridging hydrogen.

However, an investigation of **6** led to a different result. Two regioisomers, **17** and **18**, were examined. In **18**, a hydrogen atom transfer from the B atom attacked by the nucleophile to an adjacent B atom was assumed, since an excessively high coordination number for the former results otherwise. The formation of both adducts, **17** and **18**, is mildly endoergic in the gas phase, 9.3 and 10.2 kcal/mol, respectively (no ZPE), and is nearly thermoneutral in solution. When deprotonation at the C atom is followed by energy optimization, both **17** and **18** lose a Cl^- anion, but otherwise they behave differently. While **17** also loses trimethylamine with a simultaneous rearrangement of the carborane cage to **1**, in **18** trimethylamine remains attached to the boron cage and the *nido* anion **19** is formed. This is related to the observed *closo*-**16** by a net loss of two hydrogen atoms, which presumably could occur by a mechanism similar to the experimentally observed conversion of **3** to **13** mentioned above. The intermediacy of **6** in the proposed reaction mechanism thus accounts naturally for the formation of 2-substituted derivatives of **1** as byproducts in the carbene insertion reaction (Scheme 1).

DISCUSSION

At this time it would be difficult to find a more accurate method of computation than DFT that would be readily applicable to molecules of this size. Recent applications of DFT methods to borane chemistry, for example B3LYP/6-31G(d) calculations on the neutral hypercloso boron hydrides B_nH_n [29], gave encouraging results, and we believe that our results are meaningful, although small energy differences obviously cannot be trusted.

A partial check of the reliability of our results is provided by a comparison of the computed and experimental geometries of **2** and **3**. The experimental boron–boron distances within the cage of **2** in crystalline PMe_3H^+[*nido*-$B_{11}H_{14}$]$^-$ vary from 1.747 to 1.775 Å, with an average of 1.762 Å (Fig. 1)[24]. The range of boron–boron distances calculated for isolated **2a** is 1.739 to 1.811 Å, with an average of 1.775 Å. Observed boron–boron distances around the cage opening vary from 1.875 to 1.895 Å with an average of 1.886 Å [24], compared to a range of 1.853–1.980 Å and an average of 1.923 Å

from the calculations. For isolated **2b**, calculations give a range of 1.87–1.93 Å and an average of 1.91 Å. In either case the agreement is mediocre (Fig. 1), but the differences could be partly due to the fluxional nature of **2** and to the effect of the counterion in the crystal structure. Also, the calculated equilibrium geometry is not corrected for averaging by thermal motions.

The high heat of deprotonation of **2** is consistent with MNDO proton affinities calculated previously[30] for other doubly charged boranes ($B_4H_4^{2-}$, $B_6H_6^{2-}$, $B_7H_7^{2-}$) in a study that found good agreement with observed proton affinities of neutral boranes and carboranes. A large heat of deprotonation in vacuum, 420.6 kcal/mol, is expected for **2** as a proton is abstracted from an already singly negative species, and the need for a very strong base is not surprising (the proton affinity of H^- at the present level of calculation is 443.4 kcal/mol).

The experimental geometry of **3** in a crystal of $Cs^+Me_4N^+[nido\text{-}B_{11}H_{13}]^{2-}$ is available for comparison[28] with the calculations and is in good qualitative agreement (Fig. 2): the structure has C_s symmetry with two hydrogen bridges on nonadjacent edges of the open face. Quantitative agreement of calculated and experimental interatomic distances is illustrated by comparison of boron–boron distances about the open face of the cage: the 1.80–1.89 Å range found experimentally compares well with the 1.79–1.92 Å calculated range, and the observed average is 1.84 Å *vs* 1.86 Å calculated.

The reasonable agreement of calculated and observed geometries encourages us to propose that the method of calculation is applicable. The three reaction paths from **2** to **1** appear logical and we cannot presently choose among them. The absence of a barrier for the addition of $:CCl_2$ to the strongly basic **3** is not surprising. The extremely facile loss of Cl^- to yield either **5** or **6** is analogous to the formation of $:CCl_2$ from CCl_3^-. We hesitate to attach much significance to the small difference between the two minuscule activation energies, and it may well be just a coincidence that the process predicted to be faster is the one leading to **6**, thus naturally accounting for the formation of the 2-substituted byproducts. Indeed, it is quite possible that at a better level of calculation **4** would not be a minimum at all.

Both **5** and **6** would be expected to deprotonate more readily than **2**, but since NaH is insoluble and the reaction heterogeneous, all these deprotonations are probably limited by mass transport, providing an opportunity for the trapping of **6** by a nucleophile. We suspect that the deprotonation of **6** on carbon dominates over removal of the bridging hydrogen, making the direct conversion of **6** to **1** insignificant, but cannot prove it. Then, the next species that might accumulate and be detectable in the reaction mixture are **8** and **9**, as the reaction steps in which they lose a chloride anion

are the only processes with significant calculated energy barriers in the overall reaction scheme. The resulting conversions into **10** and **11**, respectively, are more distantly related to the conversion of CCl_3^- into $:CCl_2$, but still appear plausible. The isomerization of the unusual structure **11** to the more stable **10** appears sensible as well. Once again, in view of a very small activation energy for this process it is quite conceivable that at a better level of calculation **11** will actually not be a separate minimum at all.

It is interesting that **10**, a tautomer of **1**, is predicted to be the initial product. It is much more acidic than **1** and its deprotonation to **12** in the basic medium of the reaction mixture would surely be rapid and limited only by transport to the surface of the NaH solid. Reprotonation of **12** during the workup of the reaction mixture will then produce the final product **1**.

In conclusion, while the mechanism of the conversion of **2** to **1** by insertion of dichlorocarbene remains unproven, three plausible pathways have now been identified.

This work was supported by the National Science Foundation (CHE-0140478).

REFERENCES AND NOTES

1. Strauss S. H.: *Chem. Rev. (Washington, D. C.)* **1993**, *93*, 927.
2. Reed C. A.: *Acc. Chem. Res.* **1998**, *31*, 133.
3. King B. T., Zharov I., Michl J.: *Chem. Innov.* **2001**, *31*, 23.
4. Franken A., King B. T., Rudolph J., Rao P., Noll B. C., Michl J.: *Collect. Czech. Chem. Commun.* **2001**, *66*, 1238.
5. Körbe S., Franken A., Michl J.: Unpublished results.
6. Becke A. D.: *J. Chem. Phys.* **1993**, *98*, 5648.
7. Lee C., Yang W., Parr R. G.: *Phys. Rev. B: Condens. Matter* **1988**, *37*, 785.
8. Miehlich B., Savin A., Stoll H., Preuss H.: *Chem. Phys. Lett.* **1989**, *157*, 200.
9. Ditchfield R., Hehre W. J., Pople J. A.: *J. Chem. Phys.* **1971**, *54*, 724.
10. Hehre W. J., Ditchfield R., Pople J. A.: *J. Chem. Phys.* **1972**, *56*, 2257.
11. Hariharan P. C., Pople J. A.: *Mol. Phys.* **1974**, *27*, 209.
12. Gordon M. S.: *Chem. Phys. Lett.* **1980**, *76*, 163.
13. Hariharan P. C., Pople J. A.: *Theor. Chim. Acta* **1973**, *28*, 213.
14. The functional was used as implemented in Gaussian 98 (ref.[17]): $0.5E_x^{HF} + 0.5E_x^{LSDA} + 0.5\Delta E_x^{BECKE88} + E_c^{LYP}$, where E_x^{HF} is Hartree–Fock exchange term, E_x^{LSDA} is the local spin density approximation exchange functional, $E_x^{BECKE88}$ is Becke's 1988 functional (Becke A. D.: *Phys. Rev. A: At., Mol., Opt. Phys.* **1988**, *38*, 3098), and E_c^{LYP} is the correlation functional of Lee, Yang, and Parr (ref.[7]).
15. Gill P. M. W., Johnson B. G., Pople J. A., Frisch M. J.: *Chem. Phys. Lett.* **1992**, *197*, 499.
16. Handy N. C., Murray C. W., Amos R. D.: *J. Phys. Chem.* **1993**, *97*, 4392.
17. Frisch M. J. *et al.*: *Gaussian 98*, Revision A.9. Gaussian, Inc., Pittsburgh (PA) 1998.
18. Carpenter J. E., Weinhold F.: *J. Mol. Struct. (THEOCHEM)* **1988**, *169*, 41.

19. Reed A. E., Curtiss L. A., Weinhold F.: *Chem. Rev. (Washington, D. C.)* **1988**, *88*, 899.
20. Onsager L.: *J. Am. Chem. Soc.* **1936**, *58*, 1486.
21. Wong M. W., Frisch M. J., Wiberg K. B.: *J. Am. Chem. Soc.* **1991**, *113*, 4776.
22. Hine J.: *J. Am. Chem. Soc.* **1950**, *72*, 2438.
23. Kirmse W.: *Carbene Chemistry*, 2nd ed., Chapter IV, p. 129. Academic Press, New York 1971.
24. Getman T. D., Krause J. A., Shore S. G.: *Inorg. Chem.* **1988**, *27*, 2398.
25. Maitre P., Eisenstein O., Michos D., Luo X. L., Siedle A. R., Wisnieski L., Zilm K. W., Crabtree R. H.: *J. Am. Chem. Soc.* **1993**, *115*, 7747.
26. Moss R. A., Munjal R. C.: *Tetrahedron Lett.* **1979**, *49*, 4721.
27. Moss R. A.: *Acc. Chem. Res.* **1980**, *13*, 58.
28. Fritchie C. J., Jr.: *Inorg. Chem.* **1967**, *6*, 1199.
29. McKee M. L., Wang Z.-X., Schleyer P. v. R.: *J. Am. Chem. Soc.* **2000**, *122*, 4781.
30. DeKock R. L., Jasperse C. P.: *Inorg. Chem.* **1983**, *22*, 3843.